

1 **Predicting the vertical low suspended sediment concentration in vegetated flow**
2 **using a random displacement model**

3 Wenxin Huai ¹, Liu Yang ¹, Wei-jie Wang ², Yakun Guo ³, Tao Wang¹

4
5 ¹State Key Laboratory of Water Resources and Hydropower Engineering Science, Wuhan
6 University, Wuhan, Hubei 430072, China.

7 ²State Key Laboratory of Simulation and Regulation of Water Cycle in River Basin, China In-
8 stitute of Water Resources and Hydropower Research, Beijing 100038, China.

9 ³Faculty of Engineering & Informatics, University of Bradford, BD7 1DP, UK.

10
11 **Highlights:**

- 12 1. The validity of random displacement model (RDM) to simulate suspended sedi-
13 ment concentration is verified.
- 14 2. A concept of integrated sediment diffusion coefficient, which is equal to a coeffi-
15 cient β multiplied by turbulent diffusion coefficient, is introduced to study the
16 dispersion and diffusion in vegetated flow.
- 17 3. Results show that β in flow with submerged canopy is larger than that in emer-
18 gent canopy flow.

19
20 **Abstract**

21 Based on the Lagrangian approach, this study proposes a random displacement
22 model (RDM) to predict the concentration of suspended sediment in vegetated steady
23 open channel flow. Validation of the method was conducted by comparing the simu-
24 lated results by using the RDM with available experimental measurements for uniform
25 open-channel flows. The method is further validated with the classical Rouse formula.
26 To simulate the important vertical dispersion caused by vegetation in the sediment-

27 laden open channel flow, a new integrated sediment diffusion coefficient is introduced
28 in this study, which is equal to a coefficient β multiplying the turbulent diffusion
29 coefficient. As such, the RDM approach for sandy flow with vegetation was established
30 for predicting the suspended sediment concentration in low-sediment-concentration
31 flow with both the emergent and submerged vegetation. The study shows that the value
32 of β for submerged vegetation flow is larger than that for emergent vegetation flow.
33 The simulated result using the RDM is in good agreement with the available experi-
34 mental data, indicating that the proposed sediment diffusion coefficient model can be
35 accurately used to investigate the sediment concentration in vegetated steady open
36 channel flow.

37

38 **Keywords:** random displacement model, suspended sediment concentration, diffusiv-
39 ity, dispersivity, vegetated sandy flows

40

41 **1 Introduction**

42 Vegetation and sediments are commonly encountered in rivers and lakes. Aquatic
43 vegetation in rivers has a great impact on the flow characteristics, especially on flow
44 velocity and turbulence (Huai et al., 2009, 2019; Liu et al. 2018). Suspended sediment
45 is of great significance to the ecology and environment in river system. The accurate
46 prediction of sediment transport in vegetated flow, however, is very complex due to
47 complicated interactions between sediments, currents, vegetation (Li et al., 2012), river
48 beds (Joanna, 2013) and riverbank (Samadi et al., 2011; Masoodi et al., 2017, 2019).
49 The sediment diffusion coefficient plays a key role on the transport of suspended sedi-
50 ment. Therefore, it is possible to study the vertical distribution of suspended sediment
51 concentration for estimating the rate of sediment transport for various flow conditions

52 (Bai & Duan, 2014).

53 Aquatic vegetation has a blocking effect on flow by increasing hydraulic resistance
54 (Gualtieri et al., 2018), thus reducing the flow velocity and transport capacity of rivers,
55 as well as complicating vertical structure of velocity and turbulence (Stone & Shen,
56 2002). In submerged vegetated flow, there exist strong velocity shear and turbulence
57 intensities at the top of the canopy due to the vertical discontinuity of the drag force
58 (Ghisalberti & Nepf, 2002; Caroppi et al., 2018). At this zone, the Kelvin-Helmholtz
59 (KH) instability exists and the vortices within the vegetation zone are mixed with the
60 overflow (Raupach et al., 1996), leading to the complex profiles of velocity and diffu-
61 sivity. Previous studies (Murphy et al., 2007; Nepf & Ghisalberti, 2008; Huai et al.,
62 2009) demonstrate that flow through submerged vegetation can be divided into several
63 layers. In this study, the three-layer model is adopted and will be described in the Sec-
64 tion 3.1. Murphy et al. (2007) conducted laboratory experiment to investigate the dif-
65 ference of diffusion coefficient between submerged vegetated flow and non-vegetated
66 flow. They found that the vertical diffusivity in submerged vegetated flow maintained
67 as a constant near the bottom of the river bed and reached the maximum at the top of
68 the vegetation and then approached to zero near the free surface. This conclusion is
69 consistent with the previous studies by Ghisalberti and Nepf (2005). The effect of emer-
70 gent vegetation on flow characteristics is relatively simpler comparing with the case of
71 submerged vegetated flow. The study of Huai et al (2009) shows that emergent vegeta-
72 tion made the vertical distribution of longitudinal velocity more uniform through the
73 water column. Nepf et al. (1997) investigated the turbulence intensity near the boundary
74 region, i.e., approximately $z < 0.10h$ (where z is the vertical coordinate and h is the
75 flow depth), which region was similar to the condition without vegetation. Their study
76 indicated that the turbulence in this region was mainly derived from the river-bed shear

77 stress rather than from the vegetation wake. In addition, the study on vegetation density
 78 and vertical diffusion coefficient shows that the vertical diffusion coefficient increases
 79 with the increase of the density for sparse vegetation. When the vegetation density is
 80 too high, however, the diffusion coefficient is closely related to the diameter and shape
 81 of the vegetation (Nepf, 1999, 2012).

82 There are two main methods to obtain the suspended sediment concentration profile,
 83 namely solving the two-phase mixing equation or sediment convection-diffusion equa-
 84 tion. Zhong et al. (2015) and Fu et al. (2005) obtained the velocity and sediment con-
 85 centration distribution by solving the two-phase mixing equation. However, most stud-
 86 ies on sediment concentration distribution are based on solving the following sediment
 87 convection-diffusion equation (Lyn, 2006; Cheng et al., 2013; Li et al., 2018):

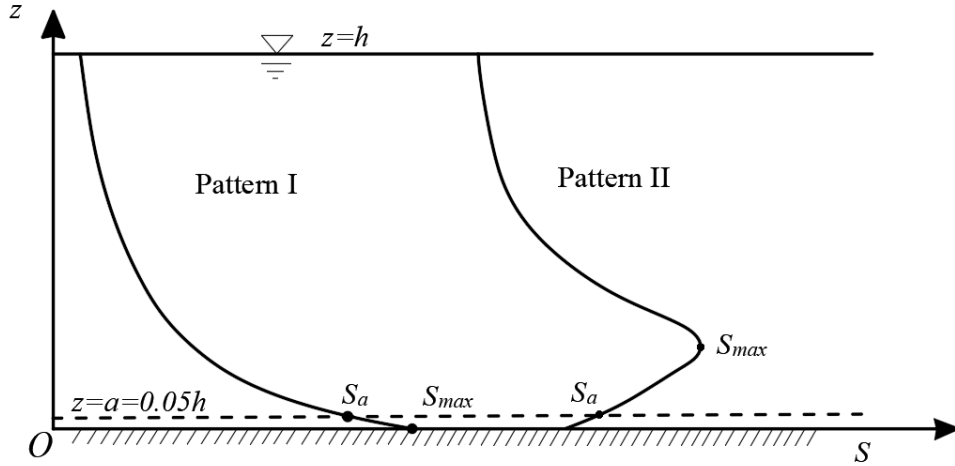
$$88 \quad K_z \frac{dS}{dz} + \omega S = 0 \quad (1)$$

89 where K_z is the vertical sediment turbulent diffusion coefficient, S is the suspended
 90 sediment concentration, and ω is the settling velocity of sediment particles. Previous
 91 studies show that there are two patterns of suspended sediment concentration profile,
 92 i.e., Pattern I (Einstein and Chien, 1955; Coleman, 1986) and Pattern II (Bouvard
 93 & Petkovic, 1985; Wang and Li, 1990). These two patterns of concentration profile are
 94 distinguished from the location of the maximum sediment concentration (S_{\max}). Two
 95 sediment concentration profile patterns are shown in a schematic diagram Fig. 1, where
 96 $a = 0.05h$ is the reference height in non-vegetated sandy flow and S_a represents the
 97 referenced sediment concentration at $z = a$. In particular, for the Pattern II concentra-
 98 tion distribution, the sediment flux generated by the turbulence, $K_z \frac{dS}{dz}$, cannot reach
 99 equilibrium with the sediment flux generated by settling velocity, ωS , in a thin region

100 near the bottom of channel. This contradicts with the sediment diffusion equation and
101 makes Eq. (1) no solution. Nevertheless, the sediment diffusion equation well illustrates
102 the movement of sediment following turbulent vortices for most conditions. Eq. (1) is
103 based on Fick's first law, therefore, the key point of solving the equation is to appropri-
104 ately determine the value of the turbulent diffusion coefficient. The effect of suspended
105 sediment on the turbulent diffusion coefficient is often reflected by the turbulent
106 Schmidt number $S_c = \frac{K_m}{K_z}$ or $\beta' = K_z / K_m$ (where K_m is the turbulent diffusion
107 coefficient) in non-vegetated sandy flow. The important coefficient β' is affected by
108 many factors, such as particle size, sediment concentration, velocity and diffusivity of
109 flow, as well as the distance from the bottom of the river-bed (Pal & Ghoshal, 2016).

110 Rouse (1937) proposed the Rouse formula by assuming $\beta' = 1$, which was later
111 proved to be incorrect. The hypothesis $\beta' = 1$ is equal to an ideal condition in which
112 the grain movement exactly follows the turbulent current. This assumption can basically
113 be considered to be correct for fine particles, however, it is incorrect for coarse sedi-
114 ments as proved by the study of Graf and Cellino (2002). Absi (2010) reasonably sim-
115 ulated the suspended sediment concentration of fine sediments with a one-dimensional
116 vertical model by assuming the coefficient to be equal to unity and only the effect of
117 particle size was considered in the study. Graf & Cellino (2002) carried out laboratory
118 experiments to show that β' is larger than unity for flow over a flat bed and is smaller
119 than unity for flow over a moveable bed form. The study by Fu et al. (2005) revealed
120 that the traditional study of sediment diffusion equations only considered the gravita-
121 tional settling and turbulent diffusion, which was only applicable to low-concentration
122 flow with fine grains. Lift force and sediment stress gradient cannot be ignored for high-

123 concentration flow. In fact, the effect of lift force and sediment stress gradient is signif-
 124 icant and should be formulated for predicting sediment dispersion in the region below
 125 $0.10h$ (Kallio & Reeks, 1989; Matida et al., 2000). This study focuses on investigating
 126 the vertical profile of low suspended sediment concentration within the vegetated uni-
 127 form flow and thus, the effects of these two items are not considered here.



128

129 **Fig. 1** Schematic diagram of two patterns of suspended sediment concentration pro-
 130 file. Pattern I: Concentration monotonously decrease from the bottom of the river to

131 the free surface (i.e. $\frac{dS}{dz} < 0$); Pattern II: The location of the maximum concentration

132 is not the bottom (i.e. $\frac{dS}{dz} > 0$ in a thin region near the bed).

133

134 When the sediment-laden flow moves through the vegetation area, the suspended
 135 sediment concentration is significantly reduced (Li et al., 2012), indicating that vegeta-
 136 tion has a great effect on the vertical suspended sediment concentration distribution.
 137 Therefore, this study is devoted to exploring the influence of vegetation on the sus-
 138 pended sediment concentration in the equilibrium open channel flow by using a La-
 139 grangian mathematical model, i.e., a random displacement model (RDM). To the best

140 knowledge of the authors, it is the first time to apply the RDM to investigate the sus-
141 pended sediment transport in vegetated, steady open channel flow. The sediment con-
142 centration profile in unsteady flow is much more complex, and there are some numeri-
143 cal models proposed for such situation (Sabbagh-Yazdi, 2013; Zhang et al., 2013; Di
144 Cristo et al., 2016), which differs from this study.

145

146 **2 Random Displacement Model (RDM)**

147 **2.1 Concept**

148 The random displacement model (RDM) is a Lagrangian method. The RDM differs
149 from the Euler method and is based on the study of particles by tracking each discrete
150 particle within the sediment-laden flow (Visser, 1997; Ross & Sharples, 2004). Cur-
151 rently, the RDM method is widely used to investigate the pollutant diffusion in open
152 channels (Salamon & Fernandez-Garcia, 2006; Liang et al, 2014; Liu et al., 2018) and
153 in the porous media (Gray et al., 2016). This is because the RDM can well represent the
154 process of the pollutant diffusion and can be used to accurately calculate the diffusivity.

155 This study applies the RDM to investigate the sediment diffusion in vegetated flow,
156 providing a new approach for study of suspended sediment concentration. In the simu-
157 lation of the sediment transport in open channel flow, sediments are represented by
158 numerous discrete particles (represented by n). The distribution of suspended sediment
159 concentration in vegetated flow is then obtained by statistical methods. For simplifica-
160 tion, this study considers a two-dimensional (2D) problem, i.e. the vertical z , and lon-
161 gitudinal x with w and u representing the time-averaged vertical and longitudinal
162 flow velocity, respectively. In each constant time step, Δt , these particles move in the
163 domain according to the following rules: The displacements (Δx and Δz) of the par-

164 ticle is decomposed into two components: the advection term and the probabilistic dif-
 165 fusion term (random displacement). The longitudinal displacement mainly depends on
 166 the time-averaged longitudinal velocity u ; while the vertical displacement depends on
 167 both the particle settling velocity (ω_i) and turbulent velocity (w'). The equations used
 168 to simulate the particle position are (Follett et al., 2016):

$$169 \quad x_{i+1} = x_i + u(z_i) \cdot \Delta t \quad (2)$$

$$170 \quad z_{i+1} = z_i + \left(\frac{dK_z}{dz}(z_i) - \omega_i \right) \Delta t + R \sqrt{2K_z(z_i) \Delta t} \quad (3)$$

171 where R is a random number conforming a normal distribution with mean 0 and
 172 standard deviation 1, the last term in Eq. (3) represents the transport by turbulent ve-

173 locity $w' = R \sqrt{\frac{2K_z(z_i)}{\Delta t}}$. The vertical transport includes a pseudo-velocity related to

174 the vertical variation in diffusivity ($\frac{dK_z}{dz}$), which prevents the artificial accumulation

175 of particles owing to low diffusivity (Boughton et al., 1987; Wilson & Yee, 2007). The

176 concentration at a certain position and time t can be obtained by counting the number

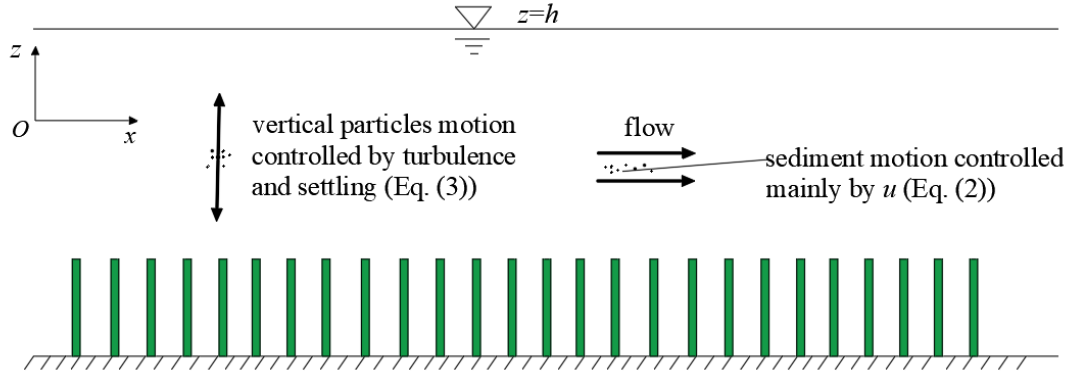
177 of particles in the volume after computing the positions of particles based on Eqs.

178 (2) and (3). The physical concept is clarified in the schematic diagram shown in Fig.

179 2. The expressions of $u(z)$ and $K_z(z)$ will differ depending on different hydraulic

180 conditions, and will be discussed in the following sections.

181



182

183 **Fig. 2** The schematic diagram of the RDM approach (governed by Eqs. (2) and (3))

184

185 According to Israelsson et al. (2006) and Follett et al. (2016), the model time step,
 186 Δt is restricted to the region of the vertical particle excursion within each time step
 187 that is much smaller than the scale of the vertical gradient in the diffusivity and velocity.
 188 This means that when the time step is too large, there will be a large deviation of the
 189 particle position calculated at the next time step by using the flow velocity and diffusion
 190 coefficient at the previous time step. Both the velocity and diffusivity vary over length
 191 scales of approximately $0.05h$. Therefore, the formula for determining time step is:

192
$$\Delta t < \min\left(\frac{0.05h}{\left|\frac{dK_z}{dz} - \omega\right|_{\max}}, \frac{(0.05h)^2}{(K_z)_{\max}}\right) \quad (4)$$

193 Assume that no bed load is present and reflecting boundary conditions are applied at
 194 the bottom of channel (Eq. (5)) and on the water surface (Eq. (6)):

195
$$z_i = -z_i, \quad z_i < 0 \quad (5)$$

196
$$z_i = 2h - z_i, \quad z_i > h \quad (6)$$

197

198 2.2 Validation of RDM using classical Rouse formula

199 To demonstrate the reliability of the RDM method for simulating sediment concen-
 200 tration, the model is firstly validated by comparing with the classic Rouse formula.

201 The velocity distribution of clear water flow is usually in the form of logarithmic
 202 distribution for uniform open-channel flow:

$$203 \quad u(z) = \frac{u_*}{k} \ln\left(\frac{30.0z}{z_0}\right) \quad (7)$$

204 where the von Karman's constant $k=0.40$ in the clear water flow, friction velocity
 205 $u_* = \sqrt{gsh}$ (g is the acceleration due to gravity, s is the slope of channel), and z_0
 206 is the roughness height.

207 Rouse assumed that the sediment diffusion coefficient was equal to the turbulent dif-
 208 fusion coefficient, i.e. $K_z = K_m$ (Rouse, 1937). K_z can be estimated from the sedi-
 209 ment diffusion equation:

$$210 \quad K_z = ku_*z \frac{h-z}{h} \quad (8)$$

211 The Rouse formula can then be expressed as:

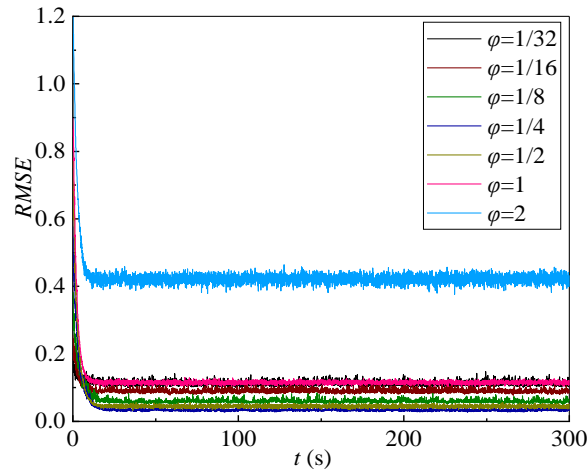
$$212 \quad \frac{S}{S_a} = \left(\frac{h-z}{z} \cdot \frac{a}{h-a}\right)^\varphi \quad (9)$$

213 where a is the reference height, generally taking as $a=0.05h$ and S_a is the sus-
 214 pended sediment concentration at the reference height. The suspension index $\varphi = \frac{\omega}{ku_*}$
 215 reflects the relative magnitude of gravity and turbulent diffusion intensity. For large
 216 φ , the gravity effect is strong and the suspended sediment will be mostly centralized
 217 not far from the bottom, leading to more uneven equilibrium sediment concentration
 218 vertically. For small φ , the turbulence intensity is strong, and more sediment can be
 219 brought to a position far away from the riverbed, which results in a much more uniform
 220 vertical equilibrium suspended sediment concentration profile. In this study, we con-

221 sider seven cases of $\varphi = \frac{1}{32}, \frac{1}{16}, \frac{1}{8}, \frac{1}{4}, \frac{1}{2}, 1$ and 2. The corresponding settling veloc-
 222 ity can be calculated as $\omega = \varphi k u_*$, the number of particles $n = 10^5$, and the time step
 223 $\Delta t = 0.05$ s, which meets the requirement of Eq. (4), $h = 0.34$ m, $z_0 = 0.01$ m and
 224 $s = 0.02$.

225 Even in the case of known velocity and turbulent field, significant computing re-
 226 sources are required to track the positions of many particles for each computational
 227 time step. Therefore, it is very important to optimize the computational time by reduc-
 228 ing the unnecessary computational time. The computational time should satisfy the
 229 equilibrium state of the sediment transport. The root-mean-square error (*RMSE*) is
 230 used to determine whether the balance of the model is statistically met. When statisti-
 231 cal balance is reached, the sediment transport can be considered to reach the equilib-
 232 rium state.

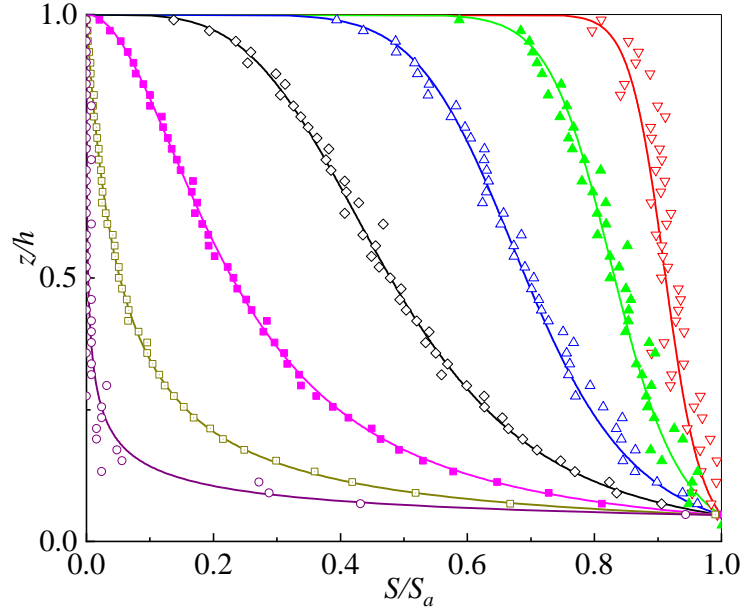
233



234

235 **Fig. 3** The variation of *RMSE* with computational time.

236



237

238 **Fig. 4** Comparison of the Rouse formula and the RDM, where solid lines indicate the

239 results of the Rouse formula and symbols indicate the simulation by the RDM. Sym-

240 bols: ∇ : $\varphi = \frac{1}{32}$; \blacktriangle : $\varphi = \frac{1}{16}$; \triangle : $\varphi = \frac{1}{8}$; \diamond : $\varphi = \frac{1}{4}$; \blacksquare : $\varphi = \frac{1}{2}$; \square : $\varphi = 1$; \circ :

241

$\varphi = 2$.

242

243 The root-mean-square error (*RMSE*) is expressed as

$$244 \quad RMSE = \sqrt{\frac{\sum_{i=1}^N (C_i - R_i)^2}{N-1}} \quad (10)$$

245 where N is the total number of sampling point, C_i is the sediment concentration

246 calculated by the RDM, and R_i is the concentration calculated by the Rouse formula

247 for the corresponding concentration position. When the *RMSE* value tends to be stable,

248 the sediment transport can be considered to have reached the equilibrium state. Fig. 3

249 shows the variation of *RMSE* with the computational time. It can be seen from Fig. 3

250 that when $t > 30$ s the simulated sediment transport for all values of φ reaches an

251 equilibrium state. The time calculated in this paper is 100 s, which meets the require-
252 ment for equilibrium state.

253 Fig. 4 is the comparison between the simulated suspended sediment concentration by
254 using the RDM method with those calculated by using the Rouse formula. Fig. 4 shows
255 that in general, the calculated suspended sediment concentration by using the RDM
256 method agrees well with those using the Rouse formula. Some relatively large discrep-
257 ancy between two methods can be found for large ϕ ($\phi=2$). Interaction of particles may
258 account for such deviation.

259

260 **2.3 Verification of RDM using the data of Einstein and Chien (1955)**

261 The Rouse formula was obtained by assuming that the sediment concentration at the
262 bottom of the river bed is infinite and zero on the water surface, which was not true.
263 The RDM method is thus further verified by comparing with the experimental data of
264 Einstein and Chien (1955), which were two-dimensional, fully developed steady open-
265 channel flows. These data are employed not only to verify the present model, but also
266 to further analyze the sediment dispersion. The experimental parameters are listed in
267 Table 1. As discussed above, the sediment concentration has an influence on the flow
268 velocity and turbulent diffusion coefficient, which will change the von Karman's con-
269 stant in the sediment laden flow. As such, the von Karman's constant obtained from
270 various experimental conditions (Einstein and Chien 1955, see Table 1) are used in the
271 simulation.

272

273 **Table 1** Flow and Sediment Characteristics in experiment of Einstein and Chien
274 (1955).

Run number	h (cm)	d (10^{-3}m)	u_* (cm/s)	$S_a(0.10h)$ (%)	ρ_s / ρ_f	k
S11	13.3	0.274	10.61	0.40	2.65	0.380
S12	13.2	0.274	10.09	1.98	2.65	0.278
S13	13.4	0.274	10.50	2.94	2.65	0.247
S14	12.4	0.274	12.12	5.10	2.65	0.255
S15	12.4	0.274	11.98	9.10	2.65	0.219

275 Note: ρ_s and ρ_f represent the density of sediment and water, respectively; d is the
276 size of sediment particle.

277

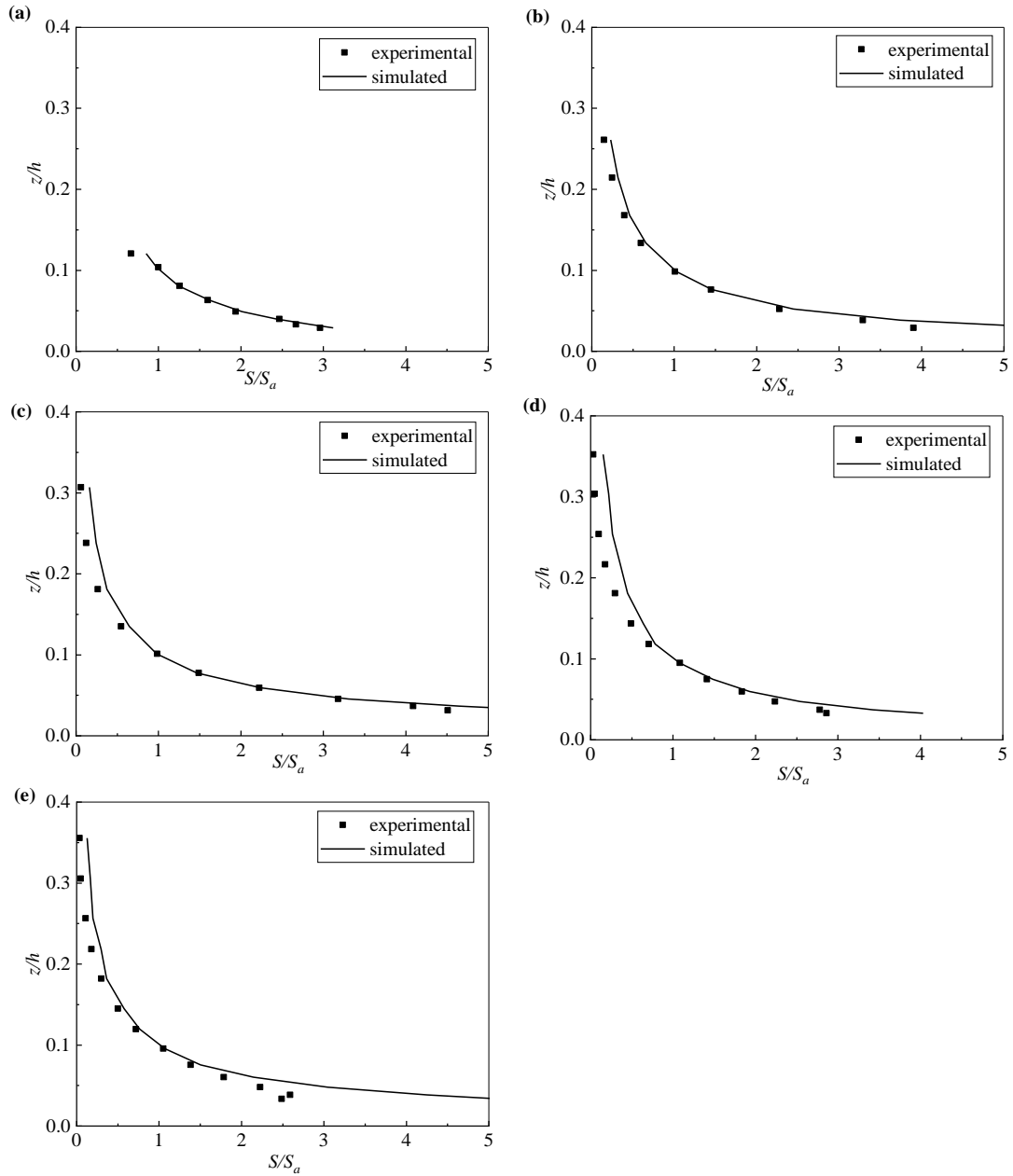
278 The particle settling velocity is very important in investigating the suspended sed-
279 iment concentration profile. The calculation formula of particle settling velocity differs
280 for various flow conditions. In this study, the formula proposed by Zhang & Xie (1989),
281 which is applicable to flow ranging from laminar to turbulent, is used to calculate the
282 particle settling velocity:

$$283 \quad \omega = \sqrt{\left(13.95 \frac{\nu}{d}\right)^2 + 1.09 \frac{\gamma_s - \gamma_f}{\gamma_f} gd} - 13.95 \frac{\nu}{d} \quad (11)$$

284 where ν represents the kinematic viscosity of water; γ_s and γ_f represent the bulk
285 density of sediment and water, respectively.

286 Sediment settling velocity can be affected by particle interaction for higher sus-
287 pended sediment concentration (Chine and Wan 1999). However, in this study the sus-
288 pended sediment concentration is low ($< 7\%$), the effect of sediment concentration on
289 the particle settling velocity can thus be ignored (Bagnold 1954).

290



291

292 **Fig. 5** Comparison of the simulated and measured suspended sediment concentration
 293 for uniform open channel flow: (a) profile S11; (b) profile S12; (c) profile S13; (d)
 294 profile S14; (e) profile S15.

295

296 Fig. 5 shows the comparison of the simulated suspended sediment concentration dis-
 297 tribution by the RDM method with the experimental results. It is seen from Fig. 5 that
 298 the model can well predict the suspended sediment concentration. While there exists

299 some slight deviation between the simulated and measured sediment concentration near
300 the bottom of the river bed where the interaction between sediments and river bed is
301 complex. Given the complexity of the problem under investigation, it can be concluded
302 that the RDM method is capable of simulating the suspended sediment transport in open
303 channel flow without vegetation with satisfactory accuracy. This provides a new
304 method for the general solution of the sediment convection-diffusion equation, which
305 is difficult to obtain analytical solution.

306

307 **3 Suspended sediment concentration in flow with vegetation**

308 This section will examine the application of the RDM method in simulating the sed-
309 iment-laden flow with vegetation. For open channel flow without aquatic vegetation,
310 the dispersion is much smaller than the diffusion, and Eq. (1) can thus be adopted to
311 describe the suspended sediment concentration. However, for open channel flow with
312 aquatic vegetation, the presence of vegetation greatly enhances the inhomogeneity of
313 vertical profile of flow velocity. In this case, the dispersion is the same order as the
314 diffusion. Therefore, it is essential to include the dispersion term in the governing equa-
315 tion. Applying the double-averaging method in vegetated steady flow (Poggi et al., 2004;
316 Termini, 2019), Eq. (1) can then be modified as:

$$317 \quad -K_z \frac{dS}{dz} + \langle w'' S'' \rangle = \omega S \quad (12)$$

318 where w'' represents the vertical time averaged velocity's deviation from the spatial
319 mean velocity $\langle w \rangle$ and S'' is the time averaged suspended sediment concentration's
320 deviation from the spatial mean concentration. Therefore, the second term on the left-
321 hand side of Eq. (12) is a dispersion term with spatial heterogeneity in the time-mean
322 velocity field. Poggi et al. (2004) demonstrated that the dispersion flux is usually
323 smaller than diffusion flux and can be ignored in clear water flow ($S'' = 0$). Eq. (12),

324 however, shows that the dispersion flux can be enhanced by the heterogeneous profile
325 of sediment concentration.

326 The dispersion flux $\langle w''S'' \rangle$ can be estimated as:

$$327 \quad \langle w''S'' \rangle = -K_{zp} \frac{dS}{dz} \quad (13)$$

328 where K_{zp} represents the sediment dispersion coefficient. Defining the integrated
329 sediment turbulent diffusion coefficient K_z' as following:

$$330 \quad K_z' = K_z + K_{zp} \approx \beta K_m \quad (14)$$

331 where the coefficient β includes the effect of diffusion and dispersion in vegetated
332 sandy flow. Many factors, such as sediment concentration, particle diameter (Pal &
333 Ghoshal, 2016) and canopy density, influence the coefficient β .

334 To propose the expression of integrated sediment turbulent diffusion based on the
335 turbulent diffusion coefficient of clear water flow and coefficient β , this study applies
336 the RDM method to simulate suspended sediment concentration of the sandy flow with
337 emergent and submerged vegetation respectively and compares the simulated results
338 with available experimental data.

339

340 **3.1 Flow with emergent vegetation**

341 Previous study (Huai et al., 2009) shows that emergent vegetation can make the
342 flow field tend to be uniform. The velocity is approximately constant in the outer region
343 and changes slightly in the viscous region near the river bed. The vegetation drag force
344 and gravity are the main effects in the outer region, where other forces are relatively
345 smaller and can be ignored. The velocity is then derived as follows:

$$346 \quad u_1 = \sqrt{\frac{2gs}{C_D a_v}} \quad (15)$$

347 where C_D is the drag coefficient ($C_D = \frac{2gs}{a_v u_1^2}$ according to Eq. (15)), a_v is the canopy frontal area per volume. Because the viscous boundary region is always thin, the
 348 outer region dominates the velocity of the flow field in emergent vegetated flow. In this
 349 study the averaged longitudinal velocity is approximated as u_1 .

351 Similarly, the turbulent diffusion coefficient of flow with emergent vegetation is
 352 generally evenly distributed. Nepf (2004) theoretically and experimentally studied the
 353 turbulent diffusion coefficient of emergent vegetation, and proposed the diffusion coefficient as follows:

$$355 \quad K_m = \alpha^3 \sqrt[3]{C_D a_v D U D} \quad (16)$$

356 where U is the averaged flow velocity in the cross-section, D is the diameter of vegetation stem and α is a proportional factor, which is taken as 0.2 for the vertical turbulent diffusion coefficient and as 0.8 for the lateral turbulent diffusion coefficient in
 358 the emergent vegetated flow.

360 To consider the effect of dispersion on the vertical suspended sediment concentration
 361 distribution in vegetated flow, substituting Eq. (16) into Eq. (14) yields:

$$362 \quad K_z' = \beta K_m = \beta \alpha^3 \sqrt[3]{C_D a_v D U D} \quad (17)$$

363

364 **Table 2** Experimental parameters, drag coefficient and determined coefficient β
 365 in emergent-canopy flow.

Run number	h (m)	D (m)	s (10^{-3})	U (m/s)	u_* (m/s)	R_e (10^4)	a_v (m^{-1})	C_D	β
D12-1	0.12	0.006	13.6	0.3343	0.1265	3.1	2.4	0.9938	2.1
D12-2	0.12	0.006	13.6	0.2918	0.1265	2.7	3.0	1.0435	2.0

D12-3	0.12	0.006	13.6	0.1690	0.1265	1.6	6.0	1.5555	2.1
D15-1	0.15	0.006	13.6	0.3321	0.1414	3.5	2.4	1.0070	2.1
D15-2	0.15	0.006	13.6	0.2932	0.1414	3.1	3.0	1.0336	2.0
D15-3	0.15	0.006	13.6	0.1700	0.1414	1.8	6.0	1.5373	2.0
D18-1	0.18	0.006	13.6	0.3436	0.1549	4.0	2.4	0.9408	2.1
D18-2	0.18	0.006	13.6	0.2947	0.1549	3.5	3.0	1.0231	2.2
D18-3	0.18	0.006	13.6	0.1692	0.1549	2.0	6.0	1.5518	2.0

366

367 We attempt to derive the vertical integrated sediment turbulent diffusion coefficient
368 of sediment-laden flow with emergent vegetation by fitting β with the experimental
369 data. To ensure the accuracy of the coefficient, interference of other factors should be
370 excluded. It is well known that the value of C_D changes slightly with the vegetation
371 density. Therefore, to eliminate the influence of the drag coefficient, we calculate C_D
372 by assuming that u_1 in Eq. (15) is equal to the averaged velocity in the cross-section
373 U . The results of the experimental parameters of the emergent canopy flow (Lu, 2008)
374 and the calculated drag coefficient are listed in Table 2 in which the size of sediment d
375 is 0.217 mm and reference height $a = 0.50h$.

376 To choose the best fitting results, the mean relative error (MRE) is used to evaluate
377 the fitting effect of the simulation and measurement:

$$378 \quad MRE = \frac{\sum \frac{|C_i - O_i|}{O_i}}{N} \times 100\% \quad (18)$$

379 where O_i is the observed sediment concentration in the experiments and definition for
380 other parameters can be found below Eq. (10). Eq. (18) shows that large MRE implies

381 that the error between simulation and observation is large. Therefore, β will be se-

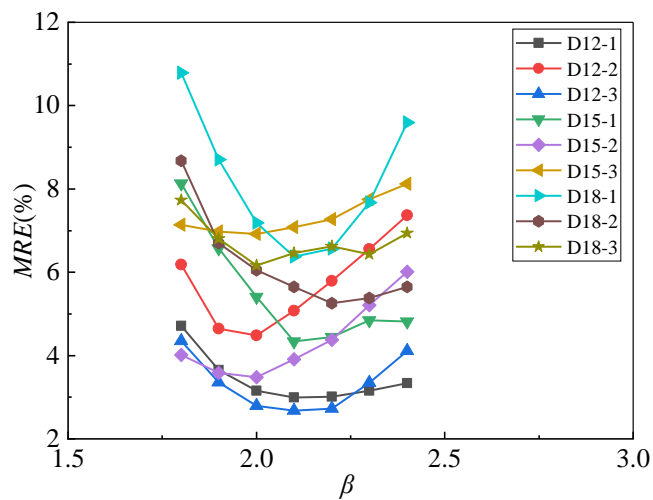
382 lected as the best-fitting coefficient for the relationship of K_z' and K_m when MRE

383 reaches the smallest value. The simulated results for MRE with β are shown in Fig.

384 6. It can be seen that the value of MRE first decreases and then increases with the in-

385 crease of β . For each case, β is then chosen at the lowest point of the curve.

386



387

388 **Fig. 6** Variation of the mean relative error (MRE) with parameter β in emergent-

389 canopy flow.

390 The coefficient β fitted from experiments is shown in Table 2 and plotted in Fig.

391 7 against experimental runs. Table 2 and Fig. 7 demonstrate that β doesn't change

392 significantly under the conditions of the experiment tested, with an averaged value of

393 2.1 for all experiments. This could be the consequence of spatial inhomogeneity en-

394 hanced by the presence of vegetation.

395 For the fitted coefficient β , the comparison between the simulated by the RDM

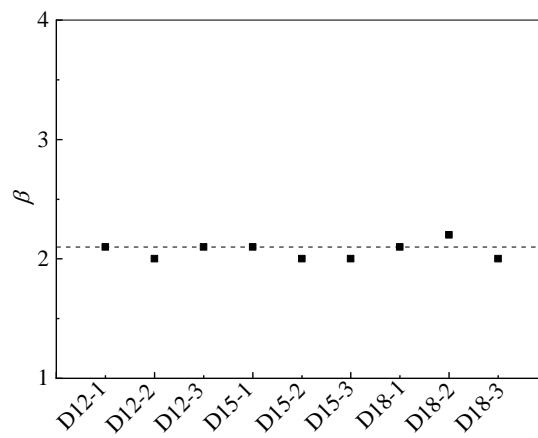
396 method and measured (Lu, 2008) suspended sediment concentration is shown in Fig.

397 8. Fig. 8 shows that the prediction of the suspended sediment concentration by the

398 proposed model, in general, agrees well with the measurements. Some discrepancy

399 in the near bed between the simulations and measurements is seen to take place. This
400 discrepancy may be ascribed to the fact that the sediment tested in the laboratory
401 experiments was not completely uniform, meaning that the suspended sediment near
402 the bottom was coarser than the median size of sediments above the bed. Eventually,
403 this will lead to the underestimation of suspended sediment concentration in the near
404 bed region by the model where the median size of sediment was used.

405



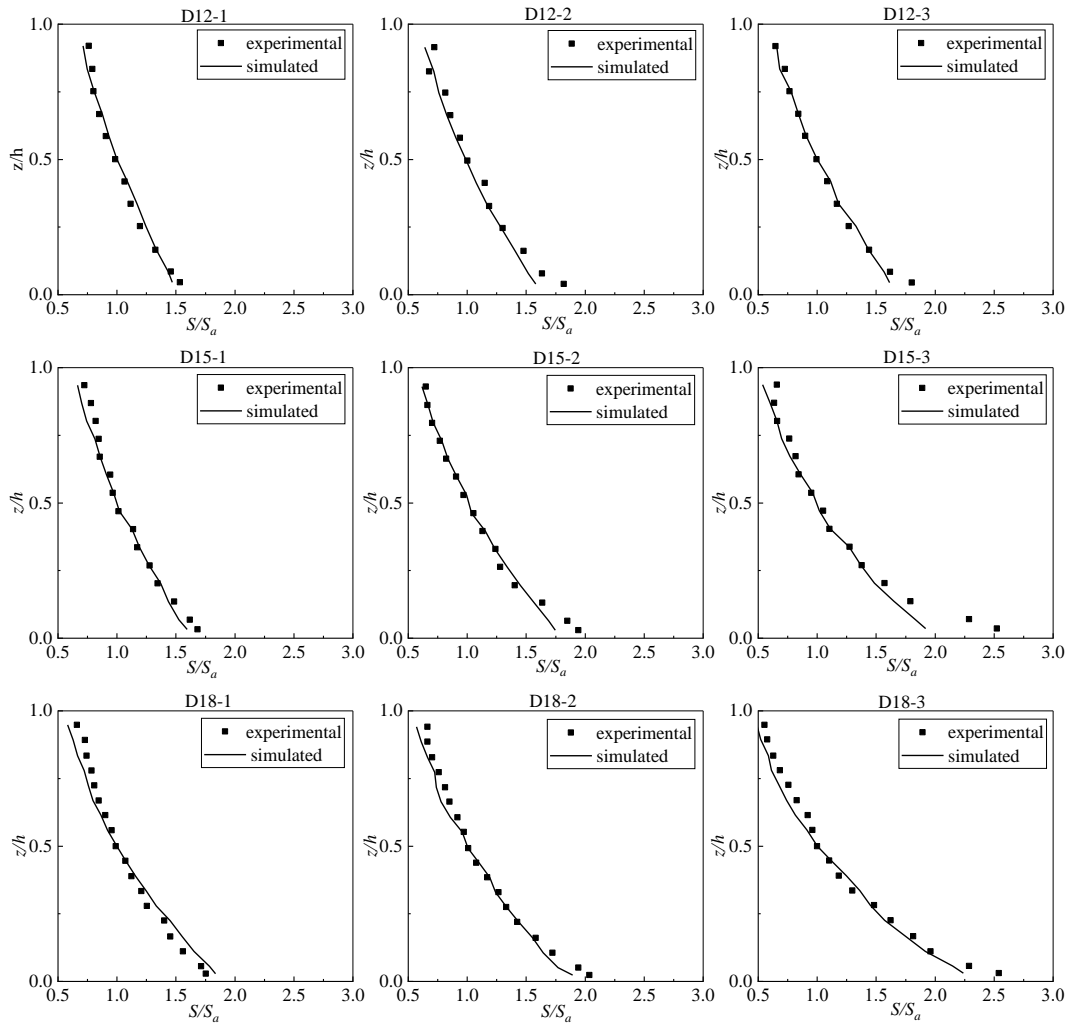
406

407 **Fig. 7** The change of β factor for nine experimental conditions in emergent-canopy

408

flow.

409



410

411 **Fig. 8** Comparison of the measured (Lu, 2008) and simulated normalized suspended
 412 sediment concentration in emergent vegetated flow.

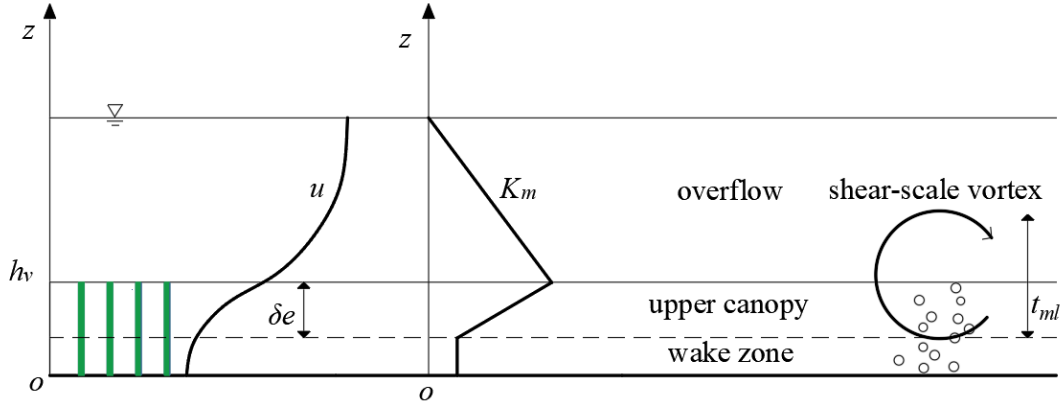
413

414 **3.2 Flow with submerged vegetation**

415 Submerged vegetation is commonly found in rivers, which greatly changes the sus-
 416 pended sediment transport and its vertical distribution. Therefore, it is of great im-
 417 portance to study the distribution of suspended sediment concentration in submerged
 418 vegetated flow. The velocity and turbulent diffusivity of flow with submerged vegeta-
 419 tion is complex. According to Nepf and Ghisalberti (2008), flow is divided into three

420 layers vertically. For a dense canopy (i.e. $a_v h_v > 0.10$ where h_v represents the veg-
 421 etation height), the flow velocity and turbulent diffusion coefficient for each layer are
 422 expressed as follows (Nepf, 2012):

423 In the overflow zone ($z \geq h_v$), the velocity profile is approximately logarithmic:
 424



425
 426 **Fig. 9** The vertical distribution of velocity and turbulent diffusivity in submerged-can-
 427 opy flow.

428

$$429 \quad u(z) = \frac{u_*}{k} \ln\left(\frac{z - z_m}{z_0}\right) \quad (19)$$

430 where z_m and z_0 are the displacement and roughness height, respectively. The dis-
 431 placement height is the centroid of momentum penetration into the canopy (Thom,
 432 1971):

$$433 \quad z_m = h_v - \frac{\delta_e}{2} \quad (20)$$

434 where the penetration length scale δ_e is the distance to which turbulent vortex pene-
 435 trates the canopy. In the range $C_D a_v h_v = 0.10$ to 0.23, the penetration length can be
 436 calculated as:

437
$$\delta_e = \frac{0.23 \pm 0.06}{C_D a_v} \quad (21)$$

438 The roughness height depends on the effective height, rather than the canopy
 439 height, so that $z_0 \propto \delta_e \propto a_v^{-1}$. For example, for $a_v h_v > 0.10$ (i.e. dense canopy),
 440 the roughness height can be evaluated as:

441
$$z_0 = \frac{0.04 \pm 0.02}{C_D a_v} \quad (22)$$

442 In the upper canopy zone ($h_v - \delta_e < z < h_v$), velocity is driven by both potential gra-
 443 dients and turbulent stress. The time-averaged velocity is:

444
$$u(z) = u_1 + (u_h - u_1) \exp(-K_u (h_v - z)) \quad (23)$$

445 where the coefficient $K_u = (8.7 \pm 1.4) C_D a_v$ according to Nepf (2012), and u_1 is the
 446 velocity in the wake zone, u_h is the velocity at $z = h$ and can be obtained from Eq.
 447 (19).

448 The third zone is the wake zone ($z \leq h_v - \delta_e$), in which the velocity u_1 is almost a
 449 constant that can be described by Eq. (15).

450 The vertical turbulent diffusion coefficient K_m is based on previous research (Mur-
 451 phy et al., 2007; Nepf & Ghisalberti, 2008). Experimental studies show that for dense
 452 vegetation the vertical vortices development is limited by the vegetation in the wake
 453 region. The vertical transport is mainly controlled by the turbulence generated by the
 454 vegetation wake. The turbulent diffusion coefficient in the wake zone is:

455
$$K_m = 0.17 u_1 D \quad (24)$$

456 The turbulence intensity reaches a maximum at the top of the canopy and then grad-
 457 ually decreases towards the water surface. The turbulent diffusion coefficient at $z = h_v$
 458 is (Ghisalberti & Nepf, 2005):

459
$$K_m \Big|_{z=h_v} = 0.032\Delta u \cdot t_{ml} \quad (25)$$

460 where Δu is the velocity difference at the water surface and the wake region of the
 461 vegetated flow (i.e. $\Delta u = u_h - u_1$), and t_{ml} is the thickness of the mixing layer (Ghi-
 462 salberti & Nepf, 2002), which is in general equal to vegetation height (i.e. $t_{ml} \sim h_v$).
 463 For simplification, we use an approximate method to express K_m : (1) calculating the
 464 maximum value of K_m using Eq. (25) and the value in the wake region using Eq. (24);
 465 (2) approximating the diffusion coefficient equal to zero at the water surface and a linear
 466 transition is assumed in the upper canopy and overflow, respectively. The vertical dis-
 467 tribution of K_m and $u(z)$ is then approximated as shown in Fig. 9.

468 To validate the model, the experiments of Lu (2008) and Wang et al. (2016) are used,
 469 whose experimental parameters are listed in Table 3. These experiments were con-
 470 ducted with low sediment-concentration. The size of sediment d and reference
 471 height are 0.217 mm and $0.50h$, respectively.

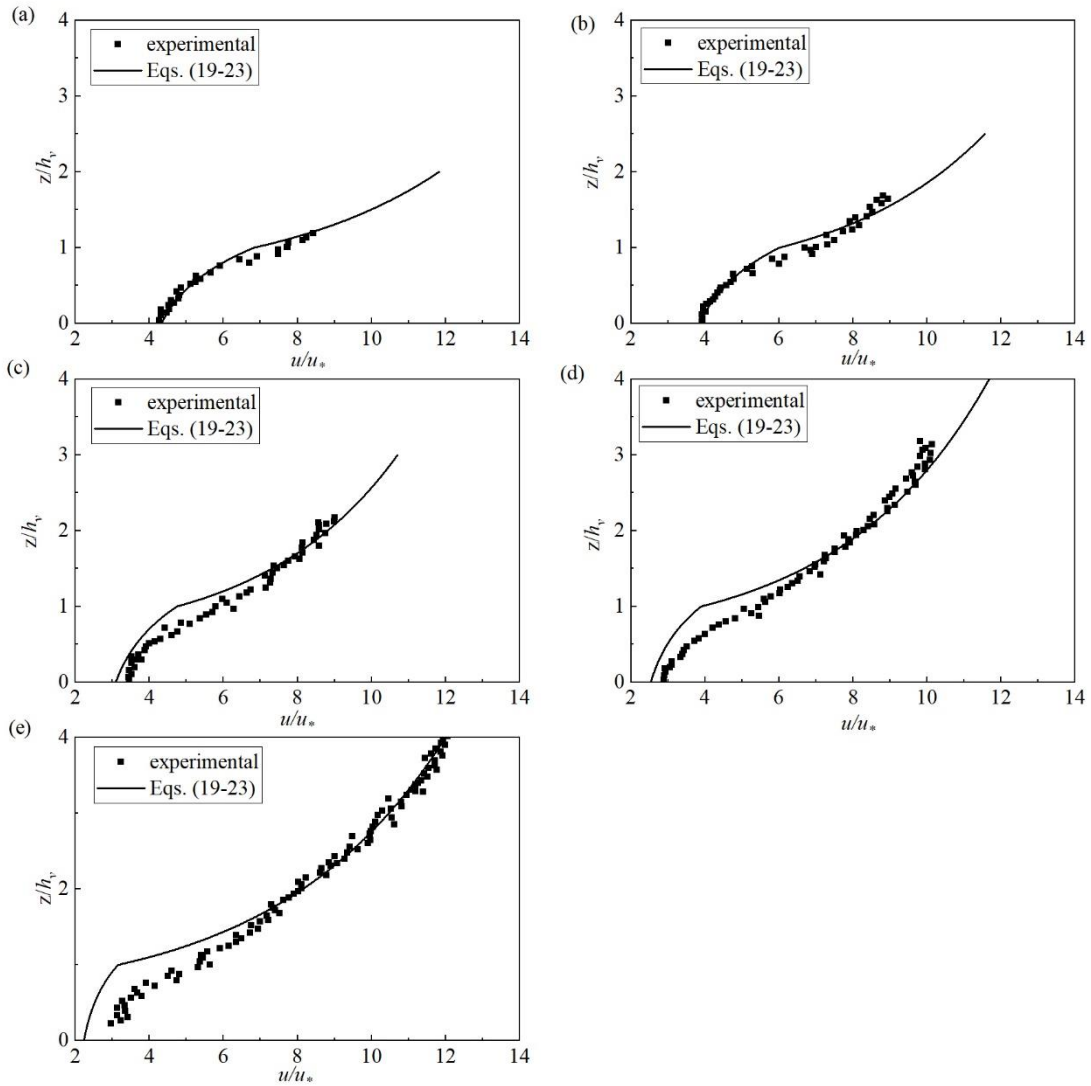
472

473 **Table 3** Experimental parameters in submerged-canopy flow.

Sources	Run number	h (cm)	h_v (cm)	D (m)	S (10^{-3})	u_* (cm/s)	Re (10^4)	a_v (m^{-1})	β
	C12	12	6	0.006	4.65	4.76	3.0	3	2.8
	C15	15	6	0.006	3.50	4.77	3.5	3	2.9
Lu	C18	18	6	0.006	2.69	5.20	4.1	3	2.8
	C24	24	6	0.006	1.35	4.45	4.1	3	2.9
	C30	30	6	0.006	0.83	3.71	4.5	3	2.7
Wang	SSW	35	25.1	0.002	0.51	2.23	0.0495	0.9	2.8

474 Note: Q and R_e represent the flow rate and Reynolds number, respectively. The R_e in
 475 Wang's experiment is stem Reynolds number, $R_e = DU / \nu$.

476



477

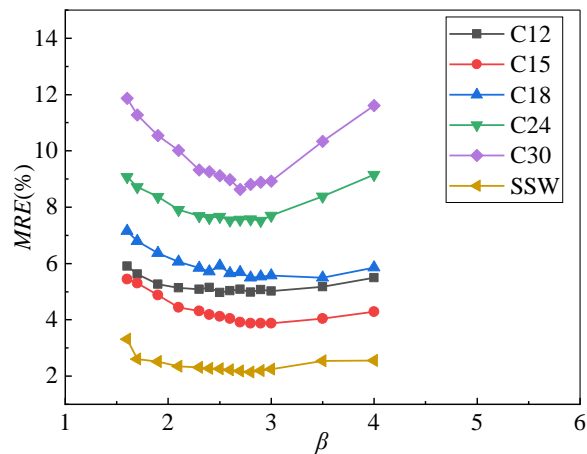
478 **Fig. 10** Comparison of the simulated (by Eqs. (19-23) and measured normalized ve-
 479 locity profiles in submerged-canopy flow: (a) profile C12; (b) profile C15; (c) profile
 480 C18; (d) profile C24; (e) profile C30.

481 The integrated sediment turbulent diffusion coefficient K_z' with submerged can-
 482 opy sandy flow can be obtained from Eq. (14). Fig. 10 shows the comparison of the
 483 calculated and measured velocity profile for various flow conditions. It is seen that the

484 simulated results agree well with the measurements, particularly in the overflow region
 485 which is less affected by canopies. Some deviation between simulation and measure-
 486 ment takes place in the wake and upper canopy regions, where the flow structure is
 487 significantly affected by wake structures induced by vegetation. The presence of sedi-
 488 ment has the effect to smoothen the vertical velocity distribution, leading to the under-
 489 estimation of Eqs. (19-23), which are obtained from clear water flow, at the region near
 490 the bed and overestimation near the water surface.

491 The simulated results of MRE with β are shown in Fig. 11. The rule of MRE and β
 492 here is the same as that in the flow with emergent canopy. Values of β can be chosen
 493 from Fig. 11 at the lowest points of each curve and are listed in Table 3 and plotted in
 494 Fig. 12. Results show that the coefficient β is almost constant with an averaged value
 495 of 2.8 for submerged vegetated sandy flow.

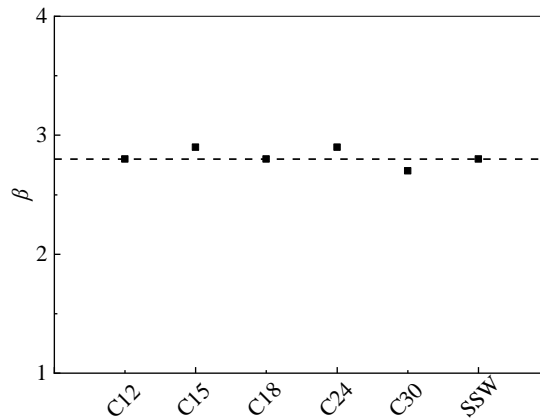
496



497

498 **Fig. 11** Variation of mean relative error (MRE) with parameter β in submerged-
 499 canopy flow.

500



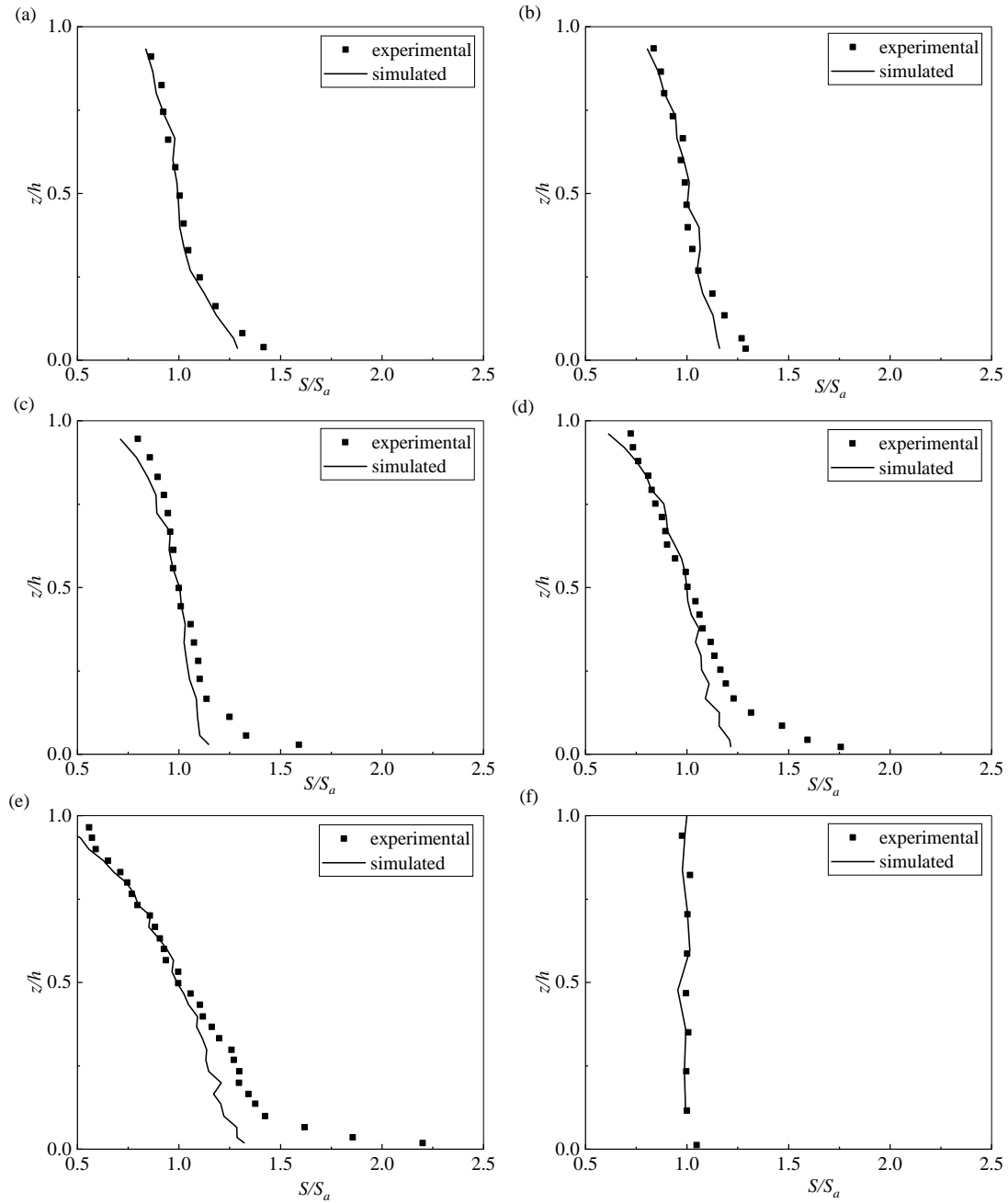
501

502 **Fig. 12** The change of factor β for six experimental conditions in submerged-
 503 canopy flow.

504

505 Fig. 13 shows the comparison of the simulated and measured normalized suspended
 506 sediment concentration for runs C12-C30 and SSW. In general, simulated suspended
 507 sediment concentration in submerged vegetation flow is in good agreement with the
 508 experimental data in almost all flow regions. Some deviation between the simulation
 509 and measurement exists near the bottom of the river bed, where the size of sediments is
 510 larger than median diameter used in model. This leads to the underestimation of sus-
 511 pended sediment concentration in the near bed region by using the model. Moreover, it
 512 is also difficult to carry out accurate measurement of suspended sediment concentration
 513 near the river bed. In general, these results demonstrate that the sediment diffusion
 514 model used in this paper can accurately simulate the concentration of suspended sedi-
 515 ment in flow with submerged vegetation.

516



517

518 **Fig. 13** Comparison of measured and simulated profiles of the normalized suspended
 519 sediment concentration in submerged-vegetation flow for different conditions: (a) pro-
 520 file C12, (b) profile C15, (c) profile C18, (d) profile C24, (e) profile C30, and (f) pro-
 521 file SSW.

522

523 4 Discussions

524 In this paper, the RDM approach is firstly applied to predict the vertical distribution

525 of suspended sediment concentration, and the settling velocity of sediment is reasona-
526 bly considered to distinguish the sediment and the pollutants, which generally ignores
527 gravity. The RDM is validated and verified by comparing the simulated results with the
528 experimental data without and with canopy flow as well as the classical Rouse formula.
529 When applying the model to steady vegetated open channel flow with low sediment
530 concentration, although microscopic movement such as collisions between sediment
531 particles or particles and vegetation are not considered, results show that the RDM
532 method can accurately simulate the flow and suspended sediment concentration profile.
533 From this perspective, the RDM is proven to be one of the effective approaches to study
534 the complex problem of suspended sediment concentration profile.

535 Owing to the presence of vegetation, the dispersion effect of sandy flow is enhanced,
536 and the mechanism of interaction between sediments, current, vegetation, and river bed
537 becomes much more complicated. The distribution of suspended sediment concentra-
538 tion mainly depends on the interaction between sediment and turbulence. In this study,
539 the RDM is applied to establish the turbulent diffusion model of the sediment-laden
540 flow by fitting coefficient β , which can well simulate the concentration distribution of
541 suspended sediment. It is reasonable to ignore the dispersion coefficient and assume
542 $\beta=1$ for low sediment concentration flow without vegetation (Dohmen-Janssen et
543 al., 2001). When aquatic vegetation exists, the dispersion, which varies greatly for dif-
544 ferent conditions, has the same order of magnitude as the turbulent diffusion and can
545 be described by Eq. (14). The value of β in Eq. (14) can be obtained by the RDM for
546 flow with both submerged and emergent vegetation. As such, the integrated sediment
547 turbulent diffusion coefficient model K_z' of the flow with vegetation can be con-
548 structed, which facilitates solving the interaction between vegetation and sandy flow.

549 The mechanism that affects the diffusion coefficient of sediment-laden flow is very

550 complicated. van Rijn (1984) proposed parameters that characterized the relationship
551 between sediment diffusion coefficient and turbulent diffusion coefficient in open chan-
552 nel flow without vegetation:

$$553 \quad K_z = \beta_p \phi K_m \quad (26)$$

554 where parameter ϕ describes the effect of the suspended sediment concentration on
555 diffusion, parameter β_p characterizes the influence of sediment particle settling ve-
556 locity on the sediment diffusion coefficient. Results of van Rijn (1984) showed that ϕ
557 was approximated to be unity in low-concentration sediment-laden flow and β_p could
558 be expressed as:

$$559 \quad \beta_p = 1 + 2 \left[\frac{\omega}{u_*} \right]^2 \quad (27)$$

560 Equation (27) shows that the value of β_p is always larger than unity and increases
561 with the increase of the particle settling velocity under the same hydraulic conditions.
562 However, the dispersion is not taken into consideration in van Rijn's study. Combining
563 with the above analysis, the coefficient β proposed in this study is more accurate as it
564 considers the influence of dispersion under the action of vegetation and sediments. The
565 results show that the dispersion effect of submerged vegetated flow $\beta=2.8$ is larger
566 than that of emergent vegetated flow $\beta=2.1$, which is consistent with the fact that
567 the vertical distribution of the velocity and diffusion coefficients in submerged vege-
568 tated flow is much more uneven than those of in emergent vegetated flow. Furthermore,
569 the modeled results imply that the value of β has no direct relation with the density of
570 vegetation in low sediment concentration flow with an emergent canopy, and is not
571 related to the density and submergence of vegetation in submerged-canopy flow. How-
572 ever, more experiments are needed to explore the law of sediment turbulent diffusivity

573 in high sediment concentration flow with canopy in which sediment particle interaction
574 should be considered.

575

576 **5 Conclusions**

577 This study is of great help in further studies of the interaction between sediments and
578 flow with vegetation. The following conclusions can be drawn from this study.

579 (1) Applying the RDM to investigate the suspended sediment concentration profile
580 in non-vegetated and vegetated open channel flow has avoided the difficulty of solving
581 the sediment diffusion equation. The simulated results are in good agreement with avail-
582 able experimental data. Since the solution of the sediment convection-diffusion equa-
583 tion is complicated when the pattern of velocity and diffusivity are complex, the use of
584 the RDM may provide a new approach to solve this problem.

585 (2) The presence of vegetation enhances the inhomogeneity of flow field, which
586 means that the dispersity cannot be ignored. This phenomenon is more obvious in sandy
587 vegetated flow. This paper proposes an integrated sediment diffusion coefficient
588 $K_z' = \beta K_m$ to express the comprehensive effect of dispersion and diffusion in the low
589 sediment concentration vegetated flow. From the simulation, β is determined as 2.1
590 for emergent-canopy sandy flow and 2.8 for submerged-canopy sandy flow.

591 (3) The solution of the parameter β significantly affects the study of the sediment
592 turbulent diffusion coefficient. To further examine the relationship between the sedi-
593 ment diffusion coefficient and turbulent diffusion coefficient, more detailed experi-
594 ments are required.

595

596 **Acknowledgements**

597 The research reported here is financially supported by the Natural Science Founda-
 598 tion of China (Nos. 51439007, 11672213, and 11872285) and the Open Funding of State
 599 Key Laboratory of Water Resources and Hydropower Engineering Science (WRHES),
 600 Wuhan University (Project No: 2018HLG01). Comments and suggestions made by the
 601 Editor, the Associate Editor and three Reviewers have greatly improved the quality of
 602 the paper.

603

604 **Notation**

605 *The following symbols are used in this article:*

a_v	canopy frontal area per volume
a	reference height
C_D	drag coefficient
C_i	suspended sediment concentration computed by RDM method
d	size of sediment particle
D	diameter of vegetation stem
g	acceleration of gravity
h	flow depth
h_v	vegetation height
k	von Karman's constant
K_m	turbulent diffusion coefficient in clear water flow
K_u	empirical coefficient
K_z	sediment turbulent diffusion coefficient
K_z'	integrated sediment turbulent diffusion coefficient
K_{zp}	sediment dispersion coefficient
MRE	mean relative error
n	the number of discrete particles
N	number of sampling point of the proposed model
O_i	observed suspended sediment concentration in experiments

R	a normally distributed random number with mean 0 and standard deviation 1
Re	Reynolds number
R_i	suspended sediment concentration computed by Rouse formula
$RMSE$	the root-mean-square error
S	suspended sediment concentration
s	slope of channel
S''	time averaged concentration's deviation from the spatial mean concentration
S_a	sediment concentration at reference height
S_c	turbulent Schmidt number
S_{max}	maximum suspended sediment concentration
t	time
t_{ml}	thickness of the mixing layer
U	average velocity in the cross-section
u_*	friction velocity
u, w	flow velocity of direction x and z , respectively
u_l	velocity in the outer region of emergent vegetated flow or velocity in the wake region of submerged vegetated flow
u_h	velocity in the water surface
w'	vertical turbulent velocity
w''	the vertical time averaged velocity's deviation from the spatial mean velocity
x, z	longitudinal and vertical coordinates, respectively
z_0	roughness height
z_m	displacement height
α	proportional factor
β	coefficient includes the effect of diffusion and dispersion in vegetated sandy flow
β_p	coefficient characterizes the influence of sediment particle settling velocity on the sediment diffusion coefficient
β'	coefficient expresses the effect of suspended sediment on the turbulent diffusion coefficient in non-vegetated sandy flow
γ_f	bulk density of water
γ_s	bulk density of sediment

δ_e	penetration length
Δt	time step
Δu	velocity difference between water surface and the wake region
Δx	displacement in the x -direction
Δz	displacement in the z -direction
ν	kinematic viscosity of fluid
φ	suspension index
ϕ	parameter
ω	settling velocity of sediment particles
$\langle w \rangle$	vertical spatial mean velocity

606

607 **References**

608 Absi, R., 2010. Concentration profiles for fine and coarse sediments suspended by
609 waves over ripples: An analytical study with the 1-DV gradient diffusion model.
610 Adv. Water Resour. 33 (4), 411 - 418.

611 <https://doi.org/10.1016/j.advwaters.2010.01.006>.

612 Bagnold, R.A., 1954. Experiments on a gravity-free dispersion of large solid spheres in
613 a Newtonian fluid under shear. Proc. R. Soc. Lond. Series A. 225, 49-63.

614 <https://doi.org/10.1098/rspa.1954.0186>.

615 Bai, Y., Duan, J. G., 2014. Simulating unsteady flow and sediment transport in vege-
616 tated channel network. J. Hydrol. 515, 90-102. [https://doi.org/10.1016/j.jhyd-](https://doi.org/10.1016/j.jhydrol.2014.04.030)

617 [drol.2014.04.030](https://doi.org/10.1016/j.jhydrol.2014.04.030) .

618 Boughton, B. A., Delaurentis, J. M., & Dunn, W. E., 1987. A stochastic model of particle
619 dispersion in the atmosphere. Bound.-Layer Meteor. 40 (1-2), 147-163.

620 <https://doi.org/10.1007/BF00140073>.

621 Bouvard, M., & Petkovic, S., 1985. Vertical dispersion of spherical, heavy particles in

622 turbulent open channel flow. *J. Hydraul. Res.* 24 (3), 221-227.
623 <https://doi.org/10.1080/00221688509499373>.

624 Caroppi, G., Gualtieri, P., Fontana, N., Giugni, M., 2018. Vegetated channel flows: tur-
625 bulence anisotropy at flow-rigid canopy interface. *Geosci.* 8(7), 259.
626 <https://doi.org/10.3390/geosciences8070259>.

627 Cheng, C., Song, Z. Y., Wang, Y. G., & Zhang, J. S., 2013. Parameterized expressions
628 for an improved Rouse equation. *Int. J. Sediment Res.* 28 (4), 523-534.
629 [https://doi.org/10.1016/S1001-6279\(14\)60010-X](https://doi.org/10.1016/S1001-6279(14)60010-X).

630 Chien, N., Wan, Z.H., 1999. *Mechanics of sediment transport*. ASCE Press. N. Y.
631 <https://doi.org/10.1061/9780784404003>.

632 Coleman N. L., (1986) Effects of suspended sediment on the open channel velocity
633 distribution. *Water Resour. Res.* 22(10), 1377-1384.
634 <https://doi.org/10.1029/WR022i010p01377>.

635 Di Cristo, C., Greco, M., Iervolino, M., Leopardi, A., & Vacca, A., 2015. Two-dimen-
636 sional two-phase depth-integrated model for transients over mobile bed. *J. Hydraul.*
637 *Eng.* ISSN: 0733-9429, 142(2), P. 04015043-1, 20.
638 [https://doi.org/10.1061/\(ASCE\)HY.1943-7900.0001024](https://doi.org/10.1061/(ASCE)HY.1943-7900.0001024).

639 Dohmen-Janssen, C. M., Hassan, W. N., & Ribberink, J. S., 2001. Mobile-bed effects
640 in oscillatory sheet flow. *J. Geophys. Res.-Oceans.* 106 (C11), 27103-27115.
641 <https://doi.org/10.1029/2000JC000513>.

642 Einstein, H.A., Chien, N., 1955. Effects of sediment concentration near the bed on the
643 velocity and sediment distribution. M.R.D. Sediment Series, Rep. No. 8, Univ. Of
644 California, Berkeley, Berkeley, Calif., and U.S. Army Corps of Engineering.

645 Follett, E., Chamecki, M., Nepf, H., 2016. Evaluation of a random displacement model
646 for predicting particle escape from canopies using a simple eddy diffusivity model.

647 Agric. For. Meteorol. 224, 40-48. <https://doi.org/10.1016/j.agrformet.2016.04.004>.

648 Fu, X., Wang, G., Shao, X., 2005. Vertical dispersion of fine and coarse sediments in
649 turbulent open-channel flows. J. Hydraul. Eng. 131 (10), 877-888.
650 [https://doi.org/10.1061/\(ASCE\)0733-9429\(2005\)131:10\(877\)](https://doi.org/10.1061/(ASCE)0733-9429(2005)131:10(877)).

651 Ghisalberti, M., Nepf, H., 2005. Mass transport in vegetated shear flows. Environ. Fluid
652 Mech. 5 (6), 527-551. <https://doi.org/10.1007/s10652-005-0419-1>.

653 Ghisalberti, M., Nepf, H. M., 2002. Mixing layers and coherent structures in vegetated
654 aquatic flows. J. Geophys. Res.-Oceans. 107 (C2), 3-1-3-11.
655 <https://doi.org/10.1029/2001JC000871>.

656 Graf, W. H., Cellino, M., 2002. Suspension flows in open channels; experimental study.
657 J. Hydraul. Res., 40 (4), 435-447. <https://doi.org/10.1080/00221680209499886>.

658 Gray, F., Cen, J., Shah, S., Crawshaw, J., Boek, E., 2016. Simulating dispersion in po-
659 rous media and the influence of segmentation on stagnancy in carbonates. Adv.
660 Water Resour. 97, 1-10. <https://doi.org/10.1016/j.advwatres.2016.08.009>.

661 Gualtieri, P., Felice, S. D., Pasquino, V., Doria, G. P., 2018. Use of conventional flow
662 resistance equations and a model for the Nikuradse roughness in vegetated flows
663 at high submergence. J. Hydrol. Hydromech. 66(1), 107-120.
664 <https://doi.org/10.1515/johh-2017-0028>.

665 Huai, W. X., Chen, Z. B., Han, J., Zeng. Y. H., 2009. Mathematical model for the flow
666 with submerged and emerged rigid vegetation. J. Hydrodyn. 21 (5), 722-729.
667 [https://doi.org/10.1016/S1001-6058\(08\)60205-X](https://doi.org/10.1016/S1001-6058(08)60205-X).

668 Huai, W. X., Zeng, Y. H., Xu, Z. G., & Yang, Z. H., 2009. Three-layer model for ver-
669 tical velocity distribution in open channel flow with submerged rigid vegetation.

670 Adv. Water Resour. 32 (4), 487-492.
671 <https://doi.org/10.1016/j.advwatres.2008.11.014>.

672 Israelsson, P. H., Kim, Y. D., Adams, E. E., 2006. A comparison of three lagrangian
673 approaches for extending near field mixing calculations. Environ. Modell. Softw.
674 21 (12), 1631 - 1649. <https://doi.org/10.1016/j.envsoft.2005.07.008>.

675 Joanna Crowe Curran, W. Cully Hession., 2013. Vegetative impacts on hydraulics and
676 sediment processes across the fluvial system. J. Hydrol. 505, 364-376.
677 <https://doi.org/10.1016/j.jhydrol.2013.10.013>.

678 Kallio, G., Reeks, M., 1989. A numerical simulation of particle deposition in turbulent
679 boundary layers. Int. J. Multiph. Flow. 15 (3), 433 - 446.
680 [https://doi.org/10.1016/0301-9322\(89\)90012-8](https://doi.org/10.1016/0301-9322(89)90012-8).

681 Li, D., Yang, Z. H., Sun, Z., Huai, W. X., Liu, J., 2018. Theoretical model of suspended
682 sediment concentration in a flow with submerged vegetation. Water. 10 (11), 1656.
683 <https://doi.org/10.3390/w10111656>.

684 Li, J. N., Yang, J. R., Luo, J., 2012. Study on the plants growth effect of the sediment-
685 laden flow turbulence characteristics. Adv. Environ. Sci. Eng. 518-523, 4771-4777.
686 <https://doi.org/10.4028/www.scientific.net/AMR.518-523.4771>.

687 Liang. D. F, Wu. X. F., 2014. A random walk simulation of scalar mixing in flows
688 through submerged vegetations. J. Hydrodyn. 26(3), 343-350.
689 [https://doi.org/10.1016/S1001-6058\(14\)60039-1](https://doi.org/10.1016/S1001-6058(14)60039-1).

690 Liu, X.N., Zhou, Q., Huang, S., Guo, Y.K. and Liu, C. 2018. Estimation of flow direc-
691 tion in meandering compound channels. J. Hydrol. 556, 143-153.

692 <https://doi.org/10.1016/j.jhydrol.2017.10.071>.

693 Liu, X. Y., Huai, W. H., Wang, Y., Yang, Z. H., Zhang, J., 2018. Evaluation of a random
694 displacement model for predicting longitudinal dispersion in flow through sus-
695 pended canopies. *Ecol. Eng.* 116, 133 - 142.
696 <https://doi.org/10.1016/j.ecoleng.2018.03.004>.

697 Lu, S. Q., 2008. Experimental study on distribution law of suspended sediment in water
698 flow of rigid plants (in Chinese), (PhD. dissertation). Hohai University, Nanjing,
699 Jiangsu, China.

700 Lyn, D. A., 2006. A similarity approach to turbulent sediment-laden flows in open
701 channels. *J. Fluid Mech.* 193 (193), 1-26.
702 <https://doi.org/10.1017/S0022112088002034>.

703 Masoodi, A., Majdzadeh Tabatabai, M.R., Noorzad, A., and Samadi, A., 2017. Effects
704 of soil physic-chemical properties on stream bank erosion induced by seepage in
705 northeastern Iran. *Hydrol. Sci. J.* 62 (16), 2597-2613.
706 <https://doi.org/10.1080/02626667.2017.1403030>.

707 Masoodi, A., Majdzadeh Tabatabai, M.R., Noorzad, A., and Samadi, A., 2019. The
708 Evaluation of Riverbank Stability under the Influence of Soil Dispersion Phenom-
709 enon- A Case Study. *J. Hydrol. Eng.* 24 (3), 05019001-1 to 05019001-10.
710 [https://doi.org/10.1061/\(ASCE\)HE.1943-5584.0001756](https://doi.org/10.1061/(ASCE)HE.1943-5584.0001756).

711 Matida, E. A., Nishino, K., Torii, K., 2000. Statistical simulation of particle deposition
712 on the wall from turbulent dispersed pipe flow. *Int. J. Heat Fluid Flow.* 21 (4), 389
713 - 402. [https://doi.org/10.1016/S0142-727X\(00\)00004-7](https://doi.org/10.1016/S0142-727X(00)00004-7).

714 Murphy, E., Ghisalberti, M., Nepf, H., 2007. Model and laboratory study of dispersion
715 in flows with submerged vegetation. *Water Resour. Res.* 43 (5), 687-696.
716 <https://doi.org/10.1029/2006WR005229>.

717 Nepf, H., Ghisalberti, M., 2008. Flow and transport in channels with submerged vege-
718 tation. *Acta Geophys.* 56 (3), 753-777. <https://doi.org/10.2478/s11600-008-0017->
719 [y](https://doi.org/10.2478/s11600-008-0017-y).

720 Nepf, H., 1999. Drag, turbulence, and diffusion in flow through emergent vegetation.
721 *Water Resour. Res.* 35 (2), 1985-1986. <https://doi.org/10.1029/1998WR900069>.

722 Nepf, H., 2004. Vegetated flow dynamics. In *The Ecogeomorphology of Tidal Marshes*
723 (eds S. Fagherazzi, M. Marani and L. K. Blum), 137-163.
724 <https://doi.org/10.1029/CE059p0137>.

725 Nepf, H., 2012. Flow and transport in regions with aquatic vegetation. *Annu. Rev. Fluid*
726 *Mech.* 44 (1), 123-142. <https://doi.org/10.1146/annurev-fluid-120710-101048>.

727 Nepf, H., Sullivan, J. A., Zavistoski, R. A., 1997. A model for diffusion within emer-
728 gent vegetation. *Limnol. Oceanogr.* 42 (8), 1735-1745.
729 <https://doi.org/10.4319/lo.1997.42.8.1735>.

730 Pal, D., Ghoshal, K., 2016. Effect of particle concentration on sediment and turbulent
731 diffusion coefficients in open-channel turbulent flow. *Environ. Earth Sci.* 75 (18),
732 1245. <https://doi.org/10.1007/s12665-016-6045-z>.

733 Poggi, D., Katul, G. G., Albertson, J. D., 2004. A note on the contribution of dispersive
734 fluxes to momentum transfer within canopies. *Bound.-Layer Meteor.* 111(3), 615-
735 621. <https://doi.org/10.1023/B:BOUN.0000016563.76874.47>.

736 Raupach, M. R., Finnigan, J. J., & Brunei, Y., 1996. Coherent eddies and turbulence in
737 vegetation canopies: The mixing-layer analogy. *Bound.-Layer Meteor.* 78 (3-4),
738 351-382. <https://doi.org/10.1007/BF00120941>.

739 Ross, O. N., Sharples, J., 2004. Recipe for 1-d lagrangian particle tracking models in
740 space-varying diffusivity. *Limnol. Oceanogr. Meth.* 2 (9), 289-302.
741 <https://doi.org/10.4319/lom.2004.2.289>.

742 Rouse, H., 1937. Modern conceptions of the mechanics of fluid turbulence. *Trans.*
743 *ASCE.* 102, 463-505.

744 Sabbagh-Yazdi, S. R., Jamshidi, M., 2013. Depth-averaged hydrodynamic model for
745 gradual breaching of embankment dams attributable to overtopping considering
746 suspended sediment transport. *J. Hydraul. Eng.* 139(6), 580-592.
747 [https://doi.org/10.1061/\(ASCE\)HY.1943-7900.0000706](https://doi.org/10.1061/(ASCE)HY.1943-7900.0000706).

748 Salamon, P., Fernandez-Garcia, D., 2006. A review and numerical assessment of the
749 random walk particle tracking method. *J. Contam. Hydrol.* 87 (3), 277-305.
750 <https://doi.org/10.1016/j.jconhyd.2006.05.005>.

751 Samadi, A., Amiri-Tokaldany, E., Davoudi, M.H., and Darby, S.E., 2011. Identifying
752 the effects of parameter uncertainty on the reliability of modeling the stability of
753 overhanging multi-layered, river banks. *Geomorphology.* 134(3-4), 483-498.
754 <https://doi.org/10.1016/j.geomorph.2011.08.004>.

755 Stone, B. M., & Shen, H. T., 2002. Hydraulic resistance of flow in channels with cylin-
756 drical roughness. *J. Hydraul. Eng.-ASCE.* 128 (5), 500-506.
757 [https://doi.org/10.1061/\(ASCE\)0733-9429\(2002\)128:5\(500\)](https://doi.org/10.1061/(ASCE)0733-9429(2002)128:5(500)).

758 Shi, H. R., Liang, X. R., Huai, W. X., Wang, Y. F., 2019. Predicting the bulk average
759 velocity of open-channel flow with submerged rigid vegetation. *J. Hydrol.* 572,
760 213-225. <https://doi.org/10.1016/j.jhydrol.2019.02.045>.

761 Termini D., 2019. Turbulent mixing and dispersion mechanisms over flexible and dense
762 vegetation. *Acta Geophys.* 67, 961-970. [https://doi.org/10.1007/s11600-019-](https://doi.org/10.1007/s11600-019-00272-8)
763 [00272-8](https://doi.org/10.1007/s11600-019-00272-8).

764 Thom, A. S., 1971. Momentum absorption by vegetation. *Q. J. R. Meteorol. Soc.* 97
765 (414), 414-428. <https://doi.org/10.1002/qj.49709741404>.

766 van Rijn, L. C., 1984. Sediment transport, part ii: Suspended load transport. *J. Hydraul.*
767 *Eng.* 110 (11), 1613-1641. [https://doi.org/10.1061/\(ASCE\)0733-](https://doi.org/10.1061/(ASCE)0733-9429(1984)110:11(1613))
768 [9429\(1984\)110:11\(1613\)](https://doi.org/10.1061/(ASCE)0733-9429(1984)110:11(1613)).

769 Visser, A., 1997. Using random walk models to simulate the vertical distribution of
770 particles in a turbulent water column. *Mar. Ecol. Prog.* 158 (8), 275-281.
771 <https://doi.org/10.3354/meps158275> .

772 Wang, G., Ni, J. R., 1990. Kinetic theory for particle concentration distribution in two-
773 phase flow. *J. Eng. Mech.* 116 (12), 2738-2748.
774 [https://doi.org/10.1061/\(ASCE\)0733-9399\(1990\)116:12\(2738\)](https://doi.org/10.1061/(ASCE)0733-9399(1990)116:12(2738)).

775 Wang, X. Y., Xie, W. M., Zhang, D., He, Q., 2016. Wave and vegetation effects on
776 flow and suspended sediment characteristics: A flume study. *Estuar. Coast. Shelf*
777 *Sci.* 182, 1-11. <https://doi.org/10.1016/j.ecss.2016.09.009>.

778 Wilson, J. D., Yee, E., 2007. A critical examination of the random displacement model
779 of turbulent dispersion. *Bound.-Layer Meteor.* 125 (3), 399-416.

- 780 <https://doi.org/10.1007/s10546-007-9201-x>.
- 781 Zhong, D. Y., Zhang, L., Wu, B. S., Wang, Y., 2015. Velocity profile of turbulent sed-
782 iment-laden flows in open-channels. *Int. J. Sediment Res.* 30 (4),
783 S1001627915000530. <https://doi.org/10.1016/j.ijsrc.2014.09.005>.
- 784 Zhang, R., Xie, J. H., 1989. River sediment dynamics (in Chinese). China Water and
785 Power Press. ISBN: 9787801244260.
- 786 Zhang, S. Y., Duan, J. G., Strelkoff, T. S., 2013. Grain-scale nonequilibrium sediment-
787 transport model for unsteady flow. *J. Hydraul. Eng.* 139(1), 22-36.
788 [https://doi.org/10.1061/\(ASCE\)HY.1943-7900.0000645](https://doi.org/10.1061/(ASCE)HY.1943-7900.0000645).